

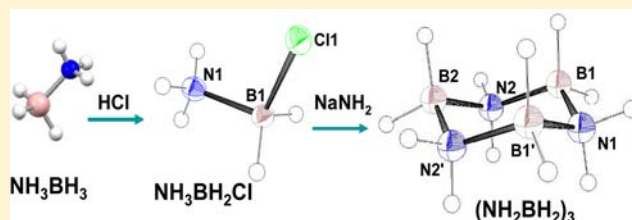
New Syntheses and Structural Characterization of $\text{NH}_3\text{BH}_2\text{Cl}$ and $(\text{BH}_2\text{NH}_2)_3$ and Thermal Decomposition Behavior of $\text{NH}_3\text{BH}_2\text{Cl}$

Hima K. Lingam, Cong Wang, Judith C. Gallucci, Xuenian Chen,* and Sheldon G. Shore*

Department of Chemistry, The Ohio State University, Columbus, Ohio 43210, United States

Supporting Information

ABSTRACT: New convenient procedures for the preparation of ammonia monochloroborane ($\text{NH}_3\text{BH}_2\text{Cl}$) and cyclotriborazane $[(\text{BH}_2\text{NH}_2)_3]$ are described. Crystal structures have been determined by single-crystal X-ray diffraction. Strong $\text{H}\cdots\text{Cl}\cdots\text{H}$ bifurcated hydrogen bonding and weak $\text{N}\cdots\text{H}\cdots\text{H}$ dihydrogen bonding are observed in the crystal structure of ammonia monochloroborane. When heated at 50°C or under vacuum, ammonia monochloroborane decomposes to $(\text{NH}_2\text{BHCl})_x$, which was characterized by NMR, elemental analysis, and powder X-ray diffraction. Redetermination of the crystal structure of cyclotriborazane at low temperature by single-crystal X-ray diffraction analysis provides accurate hydrogen positions. Similar to ammonia borane, cyclotriborazane shows extensive dihydrogen bonding of $\text{N}\cdots\text{H}\cdots\text{H}$ and $\text{B}\cdots\text{H}\cdots\text{H}$ bonds with $\text{H}^{\delta+}\cdots\text{H}^{\delta-}$ interactions in the range of 2.00–2.34 Å.

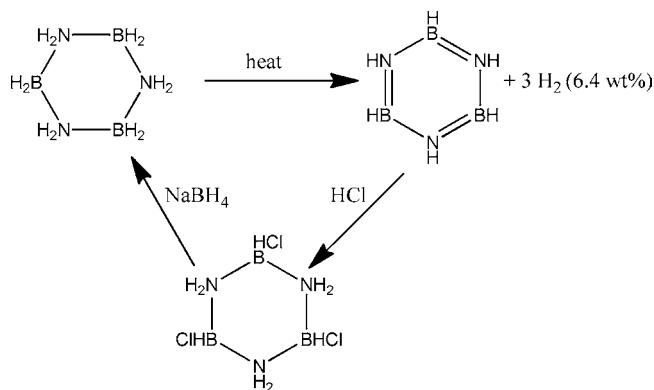


INTRODUCTION

Safe and efficient on-board hydrogen storage is a challenging issue for hydrogen to become an economically viable energy carrier.¹ Ammonia borane (AB) is a potentially excellent material for hydrogen storage with a high gravimetric hydrogen-storage capacity, 19.6 wt %.² It is nontoxic, stable in air and water, and easy to handle. Both hydridic and protonic hydrogen atoms present in ammonia borane favor hydrogen release at ambient temperatures. Hydrogen can be generated from ammonia borane by either thermal decomposition³ or hydrolysis;⁴ both of these processes are irreversible. However, thermal decomposition of AB releases hydrogen along with some unwanted boron species such as aminoborane, diborane, and borazine.³ In order to solve these problems, researchers have developed substituted ammonia borane complexes, metal amidoboranes⁵ and nitrogen-substituted ammonia boranes.⁶ Here we consider modifying ammonia borane by substituting the hydrogen atom of the BH_3 group in NH_3BH_3 with chlorine. $\text{NH}_3\text{BH}_2\text{Cl}$ is a potential precursor for the synthesis of boron nitride.⁷ Recently, we reported a convenient method for synthesis of the diammoniate of diborane starting from ammonia monochloroborane.⁸ These results triggered our interest in developing a convenient method for preparing ammonia monochloroborane and studying its crystal structure, thermal decomposition properties, and chemical reactions. Ammonia monochloroborane was first identified by ^{11}B NMR spectroscopy in the reaction between NH_3BH_3 and BCl_3 .⁹ Later it was synthesized and characterized by Ketchum et al. and employed as a precursor for the synthesis of amorphous boron nitride through pyrolysis in vacuum or in an ammonia atmosphere,⁷ but no data have been reported with respect to its structure and thermal decomposition. Among aminoborane oligomers, cyclotriborazane (hydrogen storage capacity, 13.97

wt %) has been characterized.¹⁰ Controlled dehydrogenation of cyclotriborazane to produce 6.4 wt % hydrogen and borazine has been reported.^{10a} Borazine can be hydrogenated back to cyclotriborazane and thus can possibly store hydrogen reversibly (as proposed in Scheme 1). Moreover, cyclotriborazane has higher thermal stability than ammonia borane.^{10a,f}

Scheme 1. Reversible Hydrogen Storage by Cyclotriborazane



An efficient synthesis of cyclotriborazane is required to consider it as a viable option for hydrogen storage. Here in we report a facile synthesis and structure evaluation of ammonia monochloroborane and cyclotriborazane and thermal decomposition studies of ammonia monochloroborane.

Received: October 23, 2012

Published: December 5, 2012

EXPERIMENTAL SECTION

General Procedures. All manipulations were carried out on a high-vacuum line or in a glovebox filled with high-purity nitrogen. Tetrahydrofuran (THF) and ether solvents were dried over sodium/benzophenone and freshly distilled prior to use. Ammonia (Matheson) was distilled from sodium immediately prior to use. The ^1H and $^1\text{H}\{^{11}\text{B}\}$ NMR spectra were recorded on 400 MHz spectrometers and referenced to residual solvent protons. The ^{11}B and $^{11}\text{B}\{^1\text{H}\}$ NMR spectra were obtained at 128 MHz and externally referenced to $\text{BF}_3\cdot\text{OEt}_2$ in C_6D_6 ($\delta = 0.00$ ppm). Elemental analyses were performed by Galbraith Laboratories, Inc., Knoxville, TN.

Synthesis of Ammonia Monochloroborane, $\text{NH}_3\text{BH}_2\text{Cl}$. Ammonia monochloroborane was prepared by modification of a literature procedure.⁷ NH_3BH_3 (2.00 g, 65 mmol) was placed in a two-necked 250 mL flask with a magnetic stirbar. The flask was connected to a vacuum line and evacuated, and 150 mL of Et_2O was condensed into it at -78 °C. The mixture was allowed to warm to -40 °C, and dry HCl was bubbled into the solution for 1 h with constant stirring. The reaction was monitored by ^{11}B NMR spectroscopy. When the starting material was completely consumed based upon boron signals in the ^{11}B NMR spectrum, the flow of HCl was discontinued. A very small amount of white precipitate was filtered out from the solution. Et_2O was removed from the filtrate under a dynamic vacuum to leave a white solid $\text{NH}_3\text{BH}_2\text{Cl}$ (3.93 g, yield 92%). The prepared $\text{NH}_3\text{BH}_2\text{Cl}$ was verified by ^{11}B and ^1H NMR (Figure S1 in the Supporting Information).

Synthesis of Cyclotriborazane, $(\text{BH}_2\text{NH}_2)_3$. A 100 mL THF solution of ammonia monochloroborane (1.00 g, 15 mmol) was slowly added to a suspension of NaNH_2 (0.59 g, 15 mmol) in THF. The reaction mixture was stirred for 2 h and allowed to stand for 6 h. Sodium chloride was filtered from the solution, and the solvent was evaporated under a dynamic vacuum to yield cyclotriborazane (0.30 g, yield 67%). The prepared $(\text{BH}_2\text{NH}_2)_3$ is identified by ^{11}B and $^1\text{H}\{^{11}\text{B}\}$ NMR (Figure S2 in the Supporting Information).

X-ray Crystallography. Ammonia monochloroborane (100 mg) was dissolved in 50 mL of ether and filtered, and the clear solution was concentrated to ca. 5 mL and stored at -20 °C in a freezer in a glovebox for a few days to yield small colorless crystals of ammonia monochloroborane. Single-crystal X-ray diffraction (XRD) data were collected on an Enraf-Nonius Kappa CCD diffractometer employing graphite-monochromated Mo K α radiation ($\lambda = 0.71073$ Å) at low temperature (150 K for ammonia monochloroborane and triethylamine monochloroborane and 180 K for cyclotriborazane) controlled by an Oxford Cryosystems Cryostream 700 series low-temperature system. A single crystal of $\text{NH}_3\text{BH}_2\text{Cl}$ was mounted on the tip of a glass fiber coated with Fomblin oil (a perfluoropolyether). Unit cell parameters were obtained by indexing the peaks in the first 10 frames and refined employing the whole data set. All frames were integrated and corrected for Lorentz and polarization effects using DENZO.^{11a} The data were scaled and corrected for absorption using a multiscan technique, as implemented in SADABS.¹¹ The structures of $\text{NH}_3\text{BH}_2\text{Cl}$ and $(\text{C}_2\text{H}_5)_3\text{NBH}_2\text{Cl}$ were solved by direct methods, and the structure of $(\text{NH}_2\text{BH}_2)_3$ was solved by the Patterson method; all structures were refined using SHELXTL¹² (difference electron density calculations and full-matrix least-squares refinements). All non-hydrogen atoms were located and refined anisotropically. Hydrogen atoms on boron and nitrogen atoms were located and refined isotropically, and other hydrogen atom positions were calculated by assuming standard geometries. The data collection parameters are summarized in Table 1.

Powder XRD. Powder XRD data for $\text{NH}_3\text{BH}_2\text{Cl}$, $(\text{NH}_2\text{BH}_2)_3$, and $(\text{NH}_2\text{BHCl})_x$ were collected on a Bruker D8 diffractometer (40 kV, 50 mA, Cu K α_1 radiation) equipped with a Ge(111) incident beam monochromator and a linear position-sensitive detector. The sample was ground and loaded into a 1 mm Lindeman glass capillary in an inert-atmosphere glovebox. Powder XRD data were collected over the range of $2\theta = 10$ – 70° at room temperature.

Thermal Decomposition. The thermal stability of $\text{NH}_3\text{BH}_2\text{Cl}$ and $(\text{NH}_2\text{BHCl})_x$ was studied using a Mettler-Toledo high-pressure

Table 1. Crystal Data and Structure Refinements

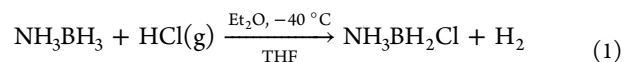
formula	H_3BNCl	$\text{H}_{12}\text{B}_3\text{N}_3$	$\text{H}_{17}\text{BC}_6\text{NCl}$
fw	65.31	86.55	149.47
cryst syst	orthorhombic	orthorhombic	monoclinic
space group	$\text{Cmc}2_1$	Pbcm	$\text{P}2_1$
Z	4	4	2
a, Å	6.703(1)	4.383(2)	6.167(1)
b, Å	5.924(1)	12.193(2)	10.707(2)
c, Å	8.292(2)	11.180(2)	7.143(1)
β , deg			113.24(3)
T, K	150(2)	180(2)	150(2)
V, Å ³	329.3(1)	597.5(2)	433.3(15)
D_{calcd} (g ³ cm ⁻³)	1.317	0.962	1.145
μ (mm ⁻¹)	0.859	0.058	0.362
λ , Å	0.71073	0.71073	0.71073
no. of reflns collected	6515	1259	7909
no. of unique reflns	251 ($R_{\text{int}} = 0.0245$)	1256 ($R_{\text{int}} = 0.0395$)	1418 ($R_{\text{int}} = 0.0240$)
R1 [$I > 2\sigma(I)$] ^a	0.0230	0.0445	0.0222
wR2 (all data) ^b	0.0442	0.1143	0.0532

^a $R_1 = \sum ||F_o| - |F_c|| / \sum |F_o|$. ^b $wR_2 = [\sum w(F_o^2 - F_c^2)^2 / \sum w(F_o^2)^2]^{1/2}$.

differential scanning calorimeter (DSC27HP) in an argon glovebox with a ramp rate of 5 °C/min. Thermogravimetric analysis (TGA) was performed on a Q5000IR analyzer (TA Instruments) coupled with a mass spectrometer (QMS 200, from Pfeiffer-Vacuum). Powder was loaded onto a quartz crucible and heated to 400 °C at a heating rate of 5 °C/min under an argon flow (flow rate, 50 cm³/min). The evolved gases from the sample in TGA were fed via a capillary heated to 200 °C into the mass spectrometer.

RESULTS AND DISCUSSION

Synthesis and Structure of Ammonia Monochloroborane. Ammonia monochloroborane was first observed by Hu and Geanangel in the reaction between ammonia borane and boron trichloride but was not isolated.⁹ The synthesis of ammonia monochloroborane was reported by Shore and co-workers by the addition of an equimolar amount of gaseous HCl to an ethereal solution of NH_3BH_3 at -196 °C followed by warming to room temperature.⁷ Ammonia monochloroborane proved to be an excellent precursor to prepare boron nitride at low temperatures (~ 600 °C). However, the original synthesis procedure requires a low reaction temperature and a special apparatus to measure the gaseous HCl; hence, it is difficult to prepare on a large scale. The modified procedure described here allows the synthesis of ammonia monochloroborane via bubbling of gaseous HCl into the ethereal solution of NH_3BH_3 with a yield of 92% (eq 1).



This new synthesis of $\text{NH}_3\text{BH}_2\text{Cl}$ is superior to the previously reported synthesis, which required measurement of the amount of HCl and employment of a vacuum line. The new procedure is essentially a simple benchtop synthesis that does not require the measurement of HCl, and the procedure can be readily scaled up. Furthermore, we found that the solvent plays a crucial role in this procedure; when THF is used instead of ether, the product forms an adduct with the solvent, which is converted to a viscous liquid during evaporation of the solvent. In dichloromethane, the reaction between ammonia borane and HCl results in the formation of a polymeric material.

Among the compounds with halogen substitution of the hydridic hydrogen of ammonia borane, only crystal structures of NH_3BCl_3 ^{13a} and NH_3BF_3 ^{13b} are reported in the literature. $\text{NH}_3\text{BH}_2\text{Cl}$ crystallizes in an orthorhombic unit cell with a $Cmc2_1$ space group (Figure 1a). Strong $\text{H}\cdots\text{Cl}$ hydrogen bonding (~ 2.54 Å) and weak $\text{H}\cdots\text{H}$ dihydrogen bonding are observed in the structure.

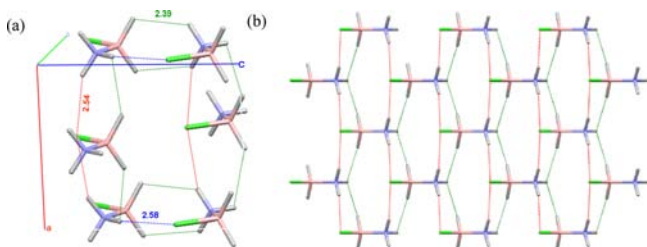


Figure 1. (a) Crystal structure of $\text{NH}_3\text{BH}_2\text{Cl}$ (B, pink; N, blue; H, gray; Cl, green). Red dotted lines indicate $\text{H}\cdots\text{Cl}\cdots\text{H}$ hydrogen bonding, blue dotted lines indicate $\text{N}-\text{H}\cdots\text{Cl}$ hydrogen bonding, and green dotted lines represent weak $\text{NH}^{\delta+}\cdots\text{H}^{\delta-}\text{B}$ dihydrogen bonding. (b) Hydrogen-bonding network in ammonia monochloroborane.

The molecules are linked via $\text{N}-\text{H}^{\delta+}\cdots\text{Cl}^{\delta-}-\text{B}$ hydrogen bonds and $\text{N}-\text{H}^{\delta+}\cdots\text{H}^{\delta-}-\text{B}$ dihydrogen bonds. The dihydrogen bond distances, shown in Figure 1a, are 2.39(2) and 2.44(4) Å (normalized based on an $\text{N}-\text{H}$ bond of 1.03 Å and a $\text{B}-\text{H}$ bond of 1.21 Å,¹⁴ longer than the $\text{H}^{\delta+}\cdots\text{H}^{\delta-}$ bond distance reported for ammonia borane (2.20 Å).¹⁴ This is possibly because of the competition between dihydrogen bonds and classical $\text{H}\cdots\text{Cl}$ hydrogen bonds. Selected bond lengths and angles are presented in Table 2. The $\text{B}-\text{N}$ bond length is

Table 2. Selected Bond Distances (Å) and Angles (deg) of H_3BNCl

Cl1–B1	1.911(3)	Cl1–B1–H1	107.0(3)
N1–H1	0.90(1)	Cl1–B1–N1	106.5(2)
N1–H2	0.86(2)	N1–B1–H1	109.0(7)
B1–H1	1.12(2)	B1–N1–H1	112.4(2)
B1–N1	1.581(3)	B1–N1–H2	107.7(2)
		N1–N1–H2	108.6(2)

1.581(3) Å, which is close to that in ammonia borane and NH_3BCl_3 [1.580(4) Å].^{13a} The $\text{N}-\text{B}-\text{Cl}$ bond angle [106.2(2)°] is similar to the $\text{N}-\text{B}-\text{Cl}$ bond angle in NH_3BCl_3 [107.6(2)°]^{13a} and also similar to the $\text{N}-\text{B}-\text{H}$ bond angles in ammonia borane [109.0(3)°]¹⁴ and methylamine borane [107.2(3)°].^{6c} The $\text{B}-\text{Cl}$ bond length is 1.911(3) Å, which is slightly longer than the observed $\text{B}-\text{Cl}$ distances in NH_3BCl_3 [1.830(4) Å]^{13a} and $\text{Et}_2\text{O}\cdot\text{BCl}_3$ [1.829(2) Å].¹⁵ The crystal structure is held together by extensive intermolecular $\text{H}\cdots\text{Cl}\cdots\text{H}$ hydrogen bonds with $\text{H}\cdots\text{Cl}$ distances of 2.54(5) and 2.58(5) Å and $\text{NH}^{\delta+}\cdots\text{H}^{\delta-}\text{B}$ dihydrogen bonds with a $\text{H}\cdots\text{H}$ bond distance of 2.39(2) Å (Figure 1b). Hydrogen bonding between metal-bound chlorine and various proton donors is well-known in the literature.^{16a–d} The $\text{H}\cdots\text{Cl}$ bond distance of 2.40 Å for compounds containing $\text{N}-\text{H}\cdots\text{Cl}$ interactions in the solid state was observed in the literature.^{16e} Each $\text{N}-\text{H}$ proton forms bifurcated hydrogen bonding with $\text{B}-\text{H}$ hydrogen and chlorine atoms. The $\text{N}-\text{H}\cdots\text{Cl}$ bond angles are [151(3)° and 158(4)°] slightly larger than those in NH_3BCl_3 ^{13a} and other $\text{M}-\text{Cl}$ complexes¹⁶ but similar to the $\text{N}-\text{H}\cdots\text{H}$ bond angle [156(3)°] observed in ammonia borane.¹⁴ The intramolecular bond distances and angles (Table 2) show that the boron and nitrogen atoms have the expected tetrahedral coordination. To determine whether the single-crystal structure of $\text{NH}_3\text{BH}_2\text{Cl}$ is the same as that of the bulk sample, powder XRD of $\text{NH}_3\text{BH}_2\text{Cl}$ was recorded at room temperature. Powder XRD patterns calculated using the refined single-crystal structure matched the experimental patterns measured at room temperature for the bulk powder, strongly suggesting no difference between the single crystal and bulk material (Figure S3 in the Supporting Information).

Thermal Decomposition. Although pyrolysis of ammonia monochloroborane was studied under vacuum and in an ammonia atmosphere for the preparation of boron nitride, the thermal decomposition process is not fully understood.⁷ It is believed that $\text{NH}_3\text{BH}_2\text{Cl}$ has a thermal decomposition pattern similar to that in the case of ammonia borane. Solid-state decomposition of ammonia borane has been reported³ to occur in stepwise reactions to release hydrogen, yielding polyaminoborane (NH_2BH_2)_x, polyiminoborane (NHBH)_x, and BN as

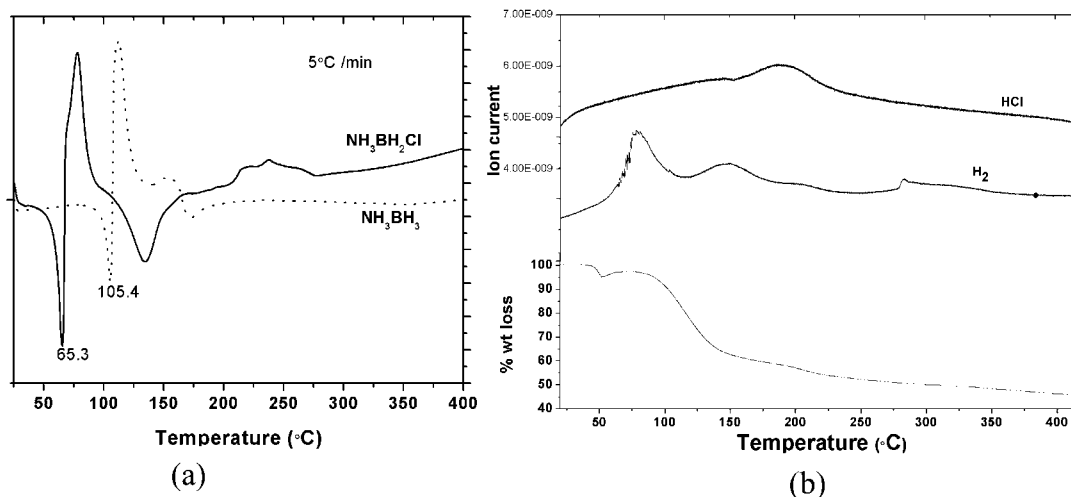


Figure 2. (a) DSC curves for $\text{NH}_3\text{BH}_2\text{Cl}$ (solid line) and ammonia borane (dashed line). (b) TGA–MS analysis of $\text{NH}_3\text{BH}_2\text{Cl}$ in the temperature range 30–400 °C with a ramp rate of 5 °C/min.

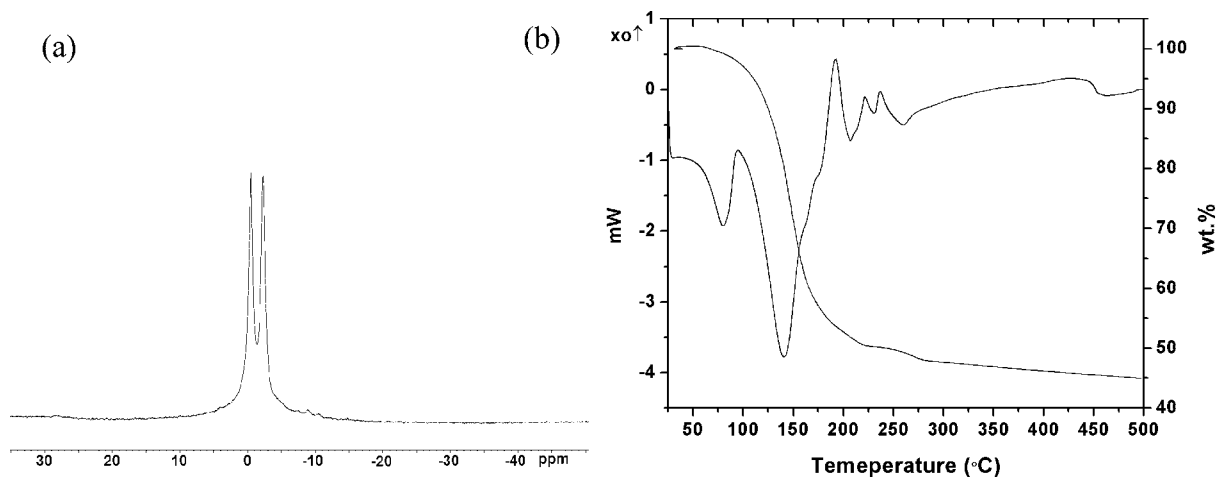
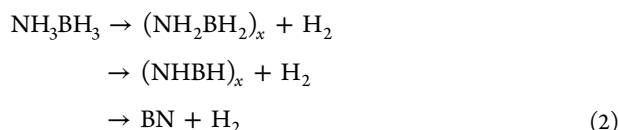
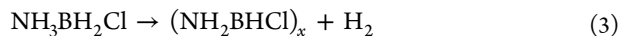


Figure 3. (a) ^{11}B NMR spectrum and (b) TGA and DSC curves of $(\text{NH}_2\text{BHCl})_x$ in the temperature range of 30–500 °C with a ramp rate of 5 °C/min.

the main solid products, as shown in eq 2, although they were not isolated and characterized.



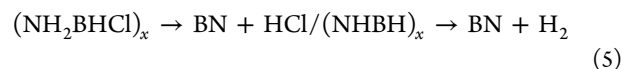
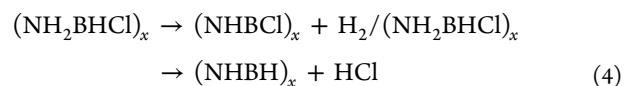
Thermal decomposition of ammonia monochloroborane was studied by differential scanning calorimetry (DSC) and TGA. Gaseous products were analyzed by mass spectrometry (MS), and solid products were examined by NMR, XRD, and elemental analysis. It was observed that ammonia monochloroborane decomposes at a lower temperature (50 °C) than ammonia borane (100 °C). Decomposition was initiated at approximately 30 °C under a static vacuum and 50 °C under an argon atmosphere. As shown in Figure 2b, thermal decomposition resulted in the generation of hydrogen only and a white solid below 80 °C. Because only hydrogen was released at the initial stage, the reaction is believed to proceed according to eq 3.



DSC curves recorded for $\text{NH}_3\text{BH}_2\text{Cl}$ and NH_3BH_3 , at a ramping rate of 5 °C/min, in an argon atmosphere are presented in Figure 2a. These depict an onset temperature at 50 °C and a second onset initiated at about 105 °C. The sample shows an endothermic melting transition at 65.3 °C, followed by exothermic decomposition at 75 °C similar to ammonia borane (105 °C, dotted line in Figure 2a) but at lower temperatures. The second step for $\text{NH}_3\text{BH}_2\text{Cl}$ is an endothermic event, whereas it is an exothermic process in ammonia borane. The mass loss profiles of $\text{NH}_3\text{BH}_2\text{Cl}$ and the m/z 2 and 36 signals recorded by the mass spectrometer during the TGA–MS experiment to 400 °C are overlaid in Figure 2b. The first weight loss (2.8 wt %) corresponds to hydrogen evolution, and the second large weight loss (52.7 wt %) is associated with both H_2 and HCl evolution; however, no other gas-phase species like NH_3 were observed.

Surprisingly, the formation of trichloroborazine was not observed during thermal decomposition of $\text{NH}_3\text{BH}_2\text{Cl}$. At higher temperatures, $\text{NH}_3\text{BH}_2\text{Cl}$ further decomposes to evolve HCl and hydrogen, and finally it forms boron nitride. On the

basis of the experimental results, decomposition of $\text{NH}_3\text{BH}_2\text{Cl}$ is believed to proceed through the following processes (eqs 3–5).



In order to identify/characterize the first decomposition product (polyaminomonochloroborane), in a separate experiment $\text{NH}_3\text{BH}_2\text{Cl}$ was decomposed overnight under vacuum at 30 °C or under an argon atmosphere at 50 °C for 6 h. During this process, -78 and -196 °C traps were used to collect evolving volatile products. Only noncondensable hydrogen was formed; no other products such as HCl and NH_3 were observed. The resulting solid was characterized by NMR, TGA, and elemental analysis. As shown in Figure 3a, a doublet at -1.2 ppm in the ^{11}B NMR spectrum in benzene confirms $-\text{BH}-$ species in the decomposed product. Attempts to obtain single crystals of the product were unsuccessful because they started decomposing in solution after a few minutes. To further verify the formation of $(\text{NH}_2\text{BHCl})_x$, elemental analysis and TGA were performed. Elem anal. Calcd for NH_2BHCl : H, 4.77; N, 22.94. Found; H, 4.66, N, 20.94 [which is consistent with the empirical formula $(\text{NH}_2\text{BHCl})_x$]; TGA and DSC curves of the decomposed product of $\text{NH}_3\text{BH}_2\text{Cl}$ at 30 °C also support the formation of a species with the empirical formula $(\text{NH}_2\text{BHCl})_x$ as shown in Figure 3b.

The total weight loss observed in TGA is 56%, and the DSC pattern is similar to that in the second step of the parent compound $\text{NH}_3\text{BH}_2\text{Cl}$, suggesting a molecule with the empirical formula $(\text{NH}_2\text{BHCl})_x$ rather than NH_3BHCl_2 . The powder XRD pattern shows the crystalline nature of the decomposed product unlike aminoborane $(\text{NH}_2\text{BH}_2)_x$ formed during decomposition of ammonia borane (Figure S4 in the Supporting Information). At the moment, we are unable to identify the molecule whether it is a $(\text{NH}_2\text{BHCl})_x$ cyclic compound or chain macromolecule.

Synthesis of Cyclotriborazane and Its Crystal Structure. Dahl and Schaeffer have reported the synthesis of cyclotriborazane by the addition of hydrogen chloride to

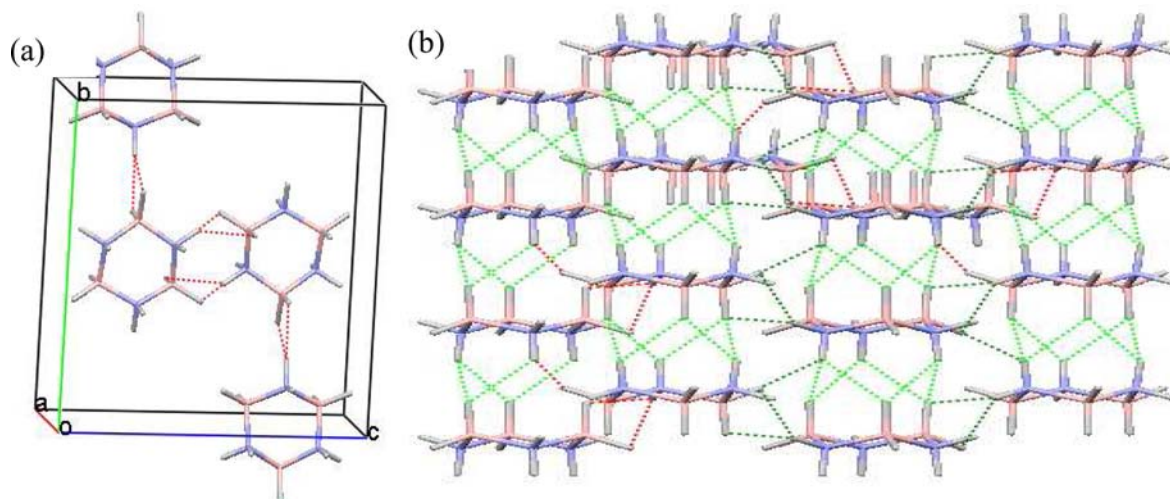
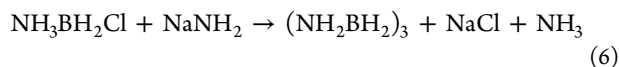


Figure 4. (a) Illustration of the crystal structure of cyclotriborazane (H, gray; B, pink; N, blue). (b) Extensive intermolecular N–H^{δ+}...H^{δ-}–B dihydrogen-bonding network in cyclotriborazane.

borazine (B₃N₃H₆) followed by reduction with sodium borohydride in diglyme with a 75% yield.^{10a} Shore et al. reported the synthesis of cyclotriborazane by reaction of the diammoniate of diborane ([[(NH₃)₂BH₂]BH₄) with either sodium acetylides^{10d} or sodium amide in liquid ammonia with low yield.^{10e} In the present method, ammonia monochloroborane was reacted with sodium amide to produce cyclotriborazane with a yield 67% (eq 6).



Electronic gas-phase calculations predicted the twisted boat form of cyclotriborazane to be more stable than the chair form¹⁷ because of intramolecular H...H interactions. High thermal stability (decomposes above 150 °C) and high heat of sublimation (25 kcal/mol)^{10b} are indicative of strong dihydrogen bonding in the crystal structure. Previously, the structure of cyclotriborazane was solved by Corfield and Shore^{10c} in the space group *Pbcm* with the molecules in the chair form. However, the hydrogen positions are not accurate because the data were collected in 1973 on an early automated Picker diffractometer at room temperature. This structure was redetermined recently at 180 K employing a Bruker automated diffractometer. Cyclotriborazane crystallizes in an orthorhombic unit cell at 180 K with space group *Pbcm* with *a* = 4.383(2) Å, *b* = 12.193(2) Å, and *c* = 11.180(2) Å, which are close to values reported by Corfield and Shore. As shown in Figure 4a, the unit cell contains four molecules of cyclotriborazane in the chair form with an average ring B–N bond length of 1.576(2) Å, not significantly different from that previously reported for the chair confirmation. The N–B–N and B–N–B bond angles in cyclotriborazane average 106.9(1)° and 115.5(2)°, respectively, against 107.2(1)° and 115.4(1)° for the corresponding angles reported earlier.^{10c,16} The H^{δ+}...H^{δ-} distances are in the range of 2.00–2.32 Å (normalized based on an N–H bond of 1.03 Å and a B–H bond of 1.21 Å).¹⁴ Selected bond angles and lengths are shown in Table S1 in the Supporting Information. Three axial BH hydrogen atoms on one molecule form bifurcated dihydrogen bonds with three axial NH hydrogen atoms on the other molecule along the same axis (Figure 4b).

Each equatorial NH hydrogen forms bifurcated dihydrogen bonding with BH₂ hydrogen atoms in neighboring molecules.

Each equatorial BH hydrogen atom forms a dihydrogen bond with an axial NH hydrogen atom in the neighboring molecules. In cyclotriborazane, the closest intermolecular bonds between adjacent molecules create three-dimensional networks in which each molecule participates in more than 20 dihydrogen bonds. The B–H...H angles are in the range of 90–170°, and the N–H...H bond angles range from 125 to 170° (Table 3).

Table 3. Geometric Characteristics of Dihydrogen Bonds in Cyclotriborazane

	H...H (Å)	∠N–H...H (deg)	∠B–H...H (deg)
H2BA–H1NA	2.06(3)	165.5(3)	99.1(3)
H1BA–H2NA	2.14(4)	142.7(3)	96.0(3)
H2BB–H1NA	2.16(4)	138.4(3)	93.9(3)
H2BB–H1NB	2.18(3)	126.7(3)	174.1(3)
H2NA–H1BB	2.24(3)	125.1(3)	172.2(3)
H1NB–H1BA	2.29(4)	133.6(3)	136.3(3)
H1BA–H2NB	2.30(2)	133.6(3)	135.6(3)
H2NB–H2BA	2.31(2)	133.1(3)	134.5(3)
H1BA–H3NB	2.32(3)	125.0(3)	135.2(3)

Powder XRD of cyclotriborazane was recorded at room temperature and confirms that the single-crystal structure of cyclotriborazane is the same as that of the bulk sample. Powder XRD patterns calculated using the refined structure matched experimental patterns measured at room temperature (Figure S5 in the Supporting Information).

Exchange Reaction with Triethylamine (Et₃N). When ammonia monochloroborane was dissolved in liquid ammonia, it formed the ionic [(NH₃)₂BH₂]Cl,⁸ whereas in Et₃N, it formed triethylamine monochloroborane (Et₃NBH₂Cl) in a substitution reaction. Evaporation of the solvent from the solution produced X-ray-quality single crystals of Et₃NBH₂Cl.^{11b} ¹¹B and ¹H NMR (Figure S6 in the Supporting Information) and melting point (43 °C) data match with the literature reported values.¹⁸ Triethylaminomonochloroborane crystallizes in a monoclinic unit cell with space group *P2*₁ and *Z* = 2. As shown in Figure 5, intramolecular bifurcated C–H...Cl...H–C hydrogen bonds with distances 2.77(8) and 2.78(8) Å and intermolecular C–H...Cl van der Waals interactions with a distance of ~3.10(4) Å were observed in the crystal structure of

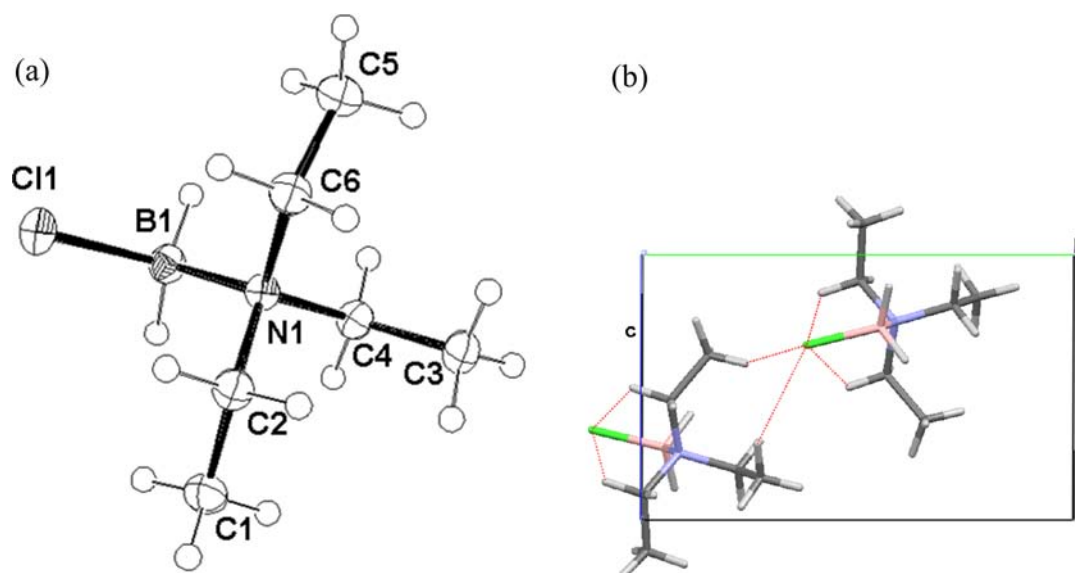


Figure 5. (a) ORTEP drawing of $\text{Et}_3\text{NBH}_2\text{Cl}$ with thermal ellipsoids plotted at the 50% probability level. (b) Crystal structure of $\text{Et}_3\text{NBH}_2\text{Cl}$ viewed along the a axis (H, gray; B, pink; C, black; N, blue; Cl, green). Red solid lines represent C–H \cdots Cl hydrogen bonding.

$\text{Et}_3\text{NBH}_2\text{Cl}$. The B–Cl bond distance is 1.882(9) Å, which is slightly shorter than the B–Cl bond distance [1.908(3) Å] in $\text{NH}_3\text{BH}_2\text{Cl}$. The B–N bond distance, 1.622(4) Å, is slightly longer than the B–N distance in $\text{NH}_3\text{BH}_2\text{Cl}$, cyclotriborazane, and ammonia borane [\sim 1.575(3) Å]. Selected bond lengths and angles are listed in Table S2 in the Supporting Information.

CONCLUSIONS

A convenient method to synthesize ammonia monochloroborane in large scale through bubbling of HCl gas into an ethereal solution of ammonia borane at -40°C has been developed. The crystal structure of ammonia monochloroborane contains extensive H \cdots Cl \cdots H bifurcated hydrogen bonding and weak dihydrogen bonding. It releases hydrogen partially below 60°C but is associated with the evolution of HCl above 80°C , which precludes it as an improved hydrogen-storage material. It can be a viable precursor for the synthesis of cyclotriborazane and amorphous boron nitride at low temperatures. The novel synthesis of cyclotriborazane might open up the possibility of using cyclotriborazane as a potential material for reversible hydrogen storage.

ASSOCIATED CONTENT

Supporting Information

X-ray crystallographic data in CIF format and powder XRD pattern, NMR, and structural information. This material is available free of charge via the Internet at <http://pubs.acs.org>.

AUTHOR INFORMATION

Corresponding Author

*E-mail: shore.1@osu.edu (S.G.S.), chen.818@osu.edu (X.C.).

Author Contributions

The manuscript was written through contributions of all authors. All authors have given approval to the final version of the manuscript.

Notes

The authors declare no competing financial interest.

ACKNOWLEDGMENTS

The authors are grateful to Prof. Thomas Evans for very valuable comments and discussions. This work was supported by the Army Research Office through Grant DAAL03-92-G-0199.

REFERENCES

- (1) (a) Schlapbach, L.; Züttel, A. *Nature* **2001**, *414*, 353–358. (b) Satyapal, S.; Petrovic, J.; Read, C.; Thomas, G.; Ordaz, G. *Catal. Today* **2007**, *120*, 246.
- (2) (a) Stephens, F. H.; Pons, V.; Baker, R. T. *Dalton Trans.* **2007**, 2613–2626. (b) Marder, T. B. *Angew. Chem., Int. Ed.* **2007**, *46*, 8116–8118. (c) Peng, B.; Chen, J. *Energy Environ. Sci.* **2008**, *1*, 479–483. (d) Hamilton, C. W.; Baker, R. T.; Staubit, A.; Manners, I. *Chem. Soc. Rev.* **2009**, *38*, 279–296. (e) Staubit, A.; Robertson, A. P. M.; Manners, I. *Chem. Rev.* **2010**, *110*, 4079–4124.
- (3) (a) Hu, M. G.; Geanangel, R. A.; Wendlandt, W. W. *Thermochim. Acta* **1978**, *23*, 249–255. (b) Baitalow, F.; Baumann, J.; Wolf, G.; Jaenicke-Rossler, K.; Leitner, G. *Thermochim. Acta* **2002**, *391*, 159–168. (c) Frueh, S.; Kellett, R.; Mallery, C.; Molter, T.; Willis, W. S.; King'ondo, C.; Suib, S. L. *Inorg. Chem.* **2011**, *50*, 783–792.
- (4) (a) Chandra, M.; Xu, Q. *J. Power Sources* **2006**, *159*, 855–860. (b) Kelly, H. C.; Marriott, V. B. *Inorg. Chem.* **1979**, *18*, 2875–2878. (c) Umegaki, T.; Yan, J.-M.; Xhang, X.-B.; Shioyama, H.; Kuriyama, N.; Xu, Q. *Int. J. Hydrogen Energy* **2009**, *34*, 2303–2311.
- (5) (a) Xiong, Z.; Yong, C. K.; Wu, G.; Chen, P.; Shaw, W.; Karkamkar, A.; Autrey, T.; Jones, M. O.; Johnson, S. R.; Edwards, P. P.; David, W. I. F. *Nat. Mater.* **2008**, *7*, 138–141. (b) Wu, H.; Zhou, W.; Yildirim, T. *J. Am. Chem. Soc.* **2008**, *130*, 14834–14839. (c) Kang, X. D.; Fang, Z. Z.; Kong, L. Y.; Cheng, H. M.; Yao, X. D.; Lu, G. Q.; Wang, P. *Adv. Mater.* **2008**, *20*, 2756–2759. (d) Diyabalanage, H. V. K.; Shrestha, R. P.; Semelsberger, T. A.; Scott, B. L.; Bowden, M. E.; Davis, B. L.; Burrell, A. K. *Angew. Chem., Int. Ed.* **2007**, *46*, 8995–8997.
- (6) (a) Hill, M. S.; Kociok-Kohn, G.; Robinson, T. P. *Chem. Commun.* **2010**, *46*, 7587–7589. (b) Beachley, O. T., Jr. *Inorg. Chem.* **1967**, *6*, 870–874. (c) Bowden, M. E.; Brown, I. W. M.; Gainsford, G. J.; Wong, H. *Inorg. Chim. Acta* **2008**, *361*, 2147–2153. (d) Staubit, A.; Soto, A. P.; Manners, I. *Angew. Chem., Int. Ed.* **2008**, *47*, 6212–6215. (e) Ryschkewitsch, G. E.; Wiggins, J. W. *Inorg. Chem.* **1970**, *9*, 314–317. (f) Aldridge, S.; Downs, A. J.; Tang, C. Y.; Parsons, S.; Clarke, M. C.; Johnstone, R. D. L.; Robertson, H. E.; Rankin, D. W. H.; Wann, D. A. *J. Am. Chem. Soc.* **2009**, *131*, 2231–43.

(7) Ketchum, D. R.; DeGraffenreid, A. L.; Niedenzu, P. M.; Shore, S. *G. J. Mater. Res.* **1999**, *14*, 1934–1938.

(8) Lingam, H. K.; Chen, X.; Shore, S. G. *Chem.—Eur. J.* **2011**, *18*, 3490–3492.

(9) Hu, M. G.; Geanangel, R. A. *Inorg. Chem.* **1979**, *18*, 3297–3301.

(10) (a) Dahl, G. H.; Schaeffer, R. *J. Am. Chem. Soc.* **1961**, *83*, 3032–3034. (b) Leavers, D. R.; Long, J. R.; Shore, S. G.; Taylor, W. J. *J. Chem. Soc. A* **1969**, 1580–1581. (c) Corfield, P. W. R.; Shore, S. G. *J. Am. Chem. Soc.* **1973**, *95*, 1480–1487. (d) Shore, S. G.; Hickam, C. W. *Inorg. Chem.* **1963**, *2*, 638–640. (e) Bøddeker, K. W.; Shore, S. G.; Bunting, R. K. *J. Am. Chem. Soc.* **1966**, *88*, 4396–4401. (f) Schellenberg, R.; Kriehme, J.; Wolf, G. *Thermochim. Acta* **2007**, *457*, 103–108.

(11) (a) Otwinowsky, Z.; Minor, W. Processing of X-ray Diffraction Data Collected in Oscillation Mode. *Methods in Enzymology*; Academic Press: New York, 1997; Vol. 276, p 307. (b) Sheldrick, G. M. *SADABS-2008/1: Bruker AXA area detector scaling and absorption correction program*; University of Göttingen: Göttingen, Germany, 2008.

(12) Sheldrick, G. M. *SHELXTL-97: A Structure Solution and Refinement Program*; University of Göttingen: Göttingen, Germany, 1998.

(13) (a) Avent, A. G.; Hitchcock, P. B.; Lappert, M. F.; Liu, D.-S.; Mignani, G.; Richard, C.; Roche, E. *J. Chem. Soc., Chem. Commun.* **1995**, 855–856. (b) Hoard, J. L.; Geller, S.; Cashin, W. M. *Acta Crystallogr.* **1951**, *4*, 396–398.

(14) Klooster, W. T.; Koetzle, T. F.; Siegbahn, P. E. M.; Richardson, T. B.; Crabtree, R. H. *J. Am. Chem. Soc.* **1999**, *121*, 6337–6343.

(15) Weinmann, M.; Nuss, J.; Jansen, M. *Acta Crystallogr.* **2006**, *E62*, o5590–o5591.

(16) (a) Aullón, G.; Bellamy, D.; Brammer, L.; Bruton, E. A.; Orpen, A. G. *Chem. Commun.* **1998**, 653–654. (b) Brammer, L.; Bruton, E. A.; Sherwood, P. *Cryst. Growth Des.* **2001**, *1*, 277–290. (c) Turner, D. R.; Smith, B.; Goeta, A. E.; Radosavljevic Evans, I.; Tocher, D. A.; Howard, J. A. K.; Steed, J. W. *CrystEngComm* **2004**, *6*, 633–641. (d) Kumar, D. K.; Das, A.; Dastidar, P. *Cryst. Growth Des.* **2005**, *5*, 651–660. (e) Hamilton, W. C.; Ibers, J. A. *Hydrogen Bonding in Solids*; W. A. Benjamin: New York, 1968.

(17) (a) Campbell, J. P.; Hwang, J.-W.; Young, V. G., Jr.; Von Dreele, R. B.; Cramer, C. J.; Gladfelter, W. L. *J. Am. Chem. Soc.* **1998**, *120*, 521–531. (b) Matus, M. H.; Anderson, K. D.; Camaioni, D. M.; Autrey, S. T.; Dixon, D. A. *J. Phys. Chem. A* **2007**, *111*, 4411–4421.

(18) (a) Nöth, H.; Beyer, H. *Chem. Ber.* **1960**, *93*, 2251–2263. (b) Faulks, J. N. G.; Greenwood, N. N.; Morris, J. H. *J. Inorg. Nucl. Chem.* **1967**, *29*, 329–333.